Perception, 2008, volume 37, pages 401 – 407

doi:10.1068/p5871

Broadening of activity with flow across neural structures

William W Lytton, Rena Orman, Mark Stewart

Downstate Medical Center, State University of New York (SUNY), 450 Clarkson Avenue, Brooklyn, New York, NY 11203, USA; e-mail: bill@neurosim.downstate.edu

Presented at Interdisciplinary Conference on Pre-Emptive Perception, Hanse Institute for Advanced Studies, Delmenhorst, Germany, 15 – 18 October 2005

Abstract. Synfire chains have long been suggested as a substrate for perception and information processing in the nervous system. However, embedding activation chains in a densely connected nervous matrix risks spread of signal that will obscure or obliterate the message. We used computer modeling and physiological measurements in rat hippocampus to assess this problem of activity broadening. We simulated a series of neural modules with feedforward propagation and random connectivity within each module and from one module to the next. We found that activity broadened as it propagated from one module to the next. This occurred over a wide array of parameters with greater broadening seen with increasing excitatory – excitatory synaptic strength. Activity broadening correlated positively with propagation velocity. Multi-electrode measurements of activity propagation in disinhibited CA1 slice demonstrated broadening of about 50% over 1 mm. Such broadening is a problem for information transfer that must be dealt with in a fully functioning nervous system.

1 Introduction

There is no general agreement on the type of code that the brain uses to transmit information about perceptual inputs or about intermediate representations leading to storage or to a behavioral output. However, most observers agree that one of the factors behind the brain's remarkable processing power is its sheer size, suggesting that information transmission and storage may well involve distributing information across many neurons and many synapses. An additional general observation that enjoys wide acceptance is the presence of parallel pathways and the presence of serial processing stations within each pathway. These design features are particularly well established in the visual system where two pathways emerge even in the retina and then become increasingly specialized with divergence into higher processing centers.

A number of coding schemes are consistent with this broad outline of the brain processing hardware: rate coding, wavefront coding, oscillation phase synchrony coding, and complex temporal coding. We will focus on the latter, and particularly on the popular model of the synfire chain, in order to illustrate some general issues of activity changing that we are exploring in simulation and physiology (Abeles 1991; Gewaltig et al 2001; Aviel et al 2003).

The synfire chain model depends on the precise timing of activity in cell ensembles. The individual neurons in these ensembles may spike simultaneously or with fixed time delays that identify them as being co-activated within the activity chain. In order for such precise activation to occur, the hypothesis envisions a coherent 'pulse packet' that propagates from one area to the next. Within each area, a particular set of cells will be activated in response to particular perceptual stimuli or particular perceptual interpretations.

We here investigate the properties of chained activity across neural modules using both computer simulation and neurophysiology. We investigate area CA1 of the hippocampus. Hippocampus has the advantage of being relatively well characterized anatomically and physiologically, and having a well-established in vitro preparation which is amenable to multi-electrode recording. Although not a primary perceptual area, hippocampus is involved in information processing involving perceptual inputs, most

clearly demonstrated in the case of place cells. In the context of pre-emptive perception, knowledge of location in space provides a strongly pertinent efference copy determining what can and what cannot be perceived.

Using simulation, we demonstrate that propagating activity has a tendency to broaden such that signals further along the chain are of greater duration and less amplitude than earlier. We find this same tendency in CA1 recordings. This tendency of chained networks to lose temporal coherence has been noted previously as a problem in the context of synfire chains or rate-coding networks (Vogels and Abbott 2005; Vogels et al 2005). We suggest that this may be a central problem in maintaining coherence of perception and information processing and in avoiding breakdown into pathological activity or failure of perceptual coherence.

2 Methods

2.1 *Modeling*

Simulations were done in NEURON (Carnevale and Hines 2006) utilizing the Artificial Cell mechanism (Lytton and Stewart 2005, 2006). The network consisted of 60 000 neurons in 10 modules. Each module consisted of 5000 excitatory (E) and 1000 inhibitory (I) neurons randomly connected with the following densities: E $\rightarrow$ E: 0.1; E $\rightarrow$ I: 0.4; I $\rightarrow$ E: 0.4; I $\rightarrow$ I: 1.0. Although densities were fixed, AMPA, NMDA, $GABA_A$, and $GABA_B$ synaptic strengths were independently varied as will be described below. Connections from one module to the next were purely feedforward and purely excitatory with connection densities of E $\rightarrow$ E: 0.2; E $\rightarrow$ I: 0.4. In addition to varying synaptic strengths, neuron excitability and neuron adaptation were also varied. The network was activated with single-spike AMPAergic stimulation of 20% of the excitatory cells in the first module.

Simulations were performed in Linux on various platforms. Multiple simulation runs were performed on an 84-node IBM-1300 Beowulf cluster.

2.2 *Physiology*

All procedures were done in accordance with SUNY Downstate regulations for animal care and use. Male Sprague–Dawley albino rats, ranging in age from 21 to 35 days, were anesthetized with halothane and decapitated. Each brain was rapidly removed from the skull and placed into iced artificial cerebrospinal fluid containing 125 mM NaCl, 2.5 mM KCl, 26 mM $NaHCO_3$, 1.25 mM NaH_2PO_4, 1.2 mM $MgCl_2$, 1.7 mM $CaCl_2$, and 11 mM glucose (pH = 7.4 when perfused with $95O_{2/5}$ tissue slicer (LeicaVT1000S). Slices were kept in oxygenated aCSF at room temperature for at least an hour before starting any recordings. All experiments were performed with a Panasonic multi-channel extracellular recording system (ALFA MED SCIENCE Co, Tokyo, Japan). Each electrode array contained 64 microelectrodes (8×8 array, 150 mm interpolar distance) made of platinum black with impedance less than 22 kOhm. A bipolar platinum/iridium stimulating electrode (impedance less than 100 kOhm) (FHC, Bowdoinham, ME, USA) was placed from the top side of the slice. A dissecting scope was used to identify slice landmarks and a digital imaging system was used to locate the recording array in relation to the slice. Signals were amplified, filtered, and digitized to disk for offline analysis.

The $GABA_A$ blocker bicuculline (50 mM, Sigma) was applied to the bath. The single stimuli were used to trigger a population burst that was observed to propagate through area CA1 from the CA3 side to the subicular side.

3 Results

A total of 34 368 simulations were run, varying parameters for intra- and inter-module excitatory and inhibitory connectivity strength, intrinsic excitability, and intrinsic adaptation mechanisms.

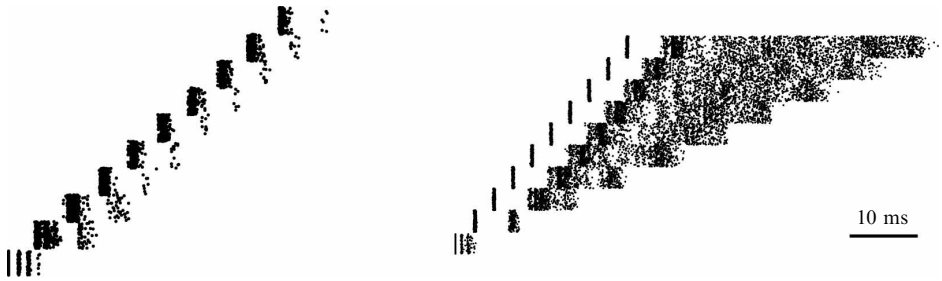

Figure 1. Activation spread in two activity-chain models. Raster plots show time of spiking with sequential activation of modules after initial triggering (lower right in each). (a) Minimal broadening is seen with weak connectivity. (b) Pronounced broadening with stronger connectivity.

Simulation of unidirectionally connected chains of modules demonstrated some broadening of activity in most cases (figure 1). This can be explained as follows. The activation of a subset of cells in module 1 activated additional neurons in module 1 (local response) while projecting to activate neurons in module 2 (propagating response). The local response persists owing to a slight imbalance between depolarizing and hyperpolarizing postsynaptic potentials (PSPs) with a preponderance of excitatory tone. As intrinsic adaptation mechanisms and $GABA_B$ tone gradually increase, they tip the balance towards hyperpolarizing influences and terminate activity. In the simulations shown, the intrinsic adaptation mechanisms played the major role, with inhibitory mechanisms contributing little (figure 2).

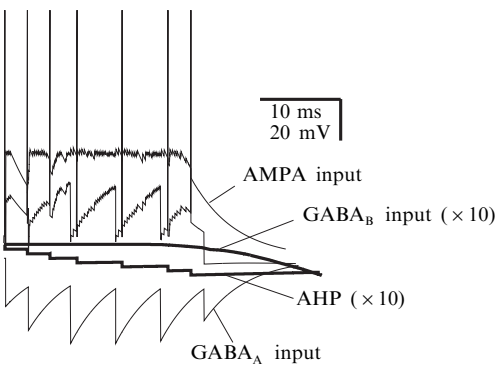

Figure 2. Activity in one neuron (top spiking trace) is sustained by a slight excess in AMPA activation over $GABA_A$ activation. After activity has been sustained for a period of time, slower mechanisms, an after-hyperpolarizing (AHP) adaptation response and a lower-amplitude $GABA_B$ response, grow and terminate activity. Note that AHP and $GABA_B$ hyperpolarizations are at $10 \times$ scale.

When one of these modules is placed in a chain, a follower module $n+1$ is influenced not only by its own intrinsic excitatory responses but is also subject to excitatory activation from prior module n. This inter-module activation is both directly excitatory (pyramidal to pyramidal) and indirectly inhibitory (pyramidal to inhibitory interneuron to pyramidal), with the excitatory response again dominating, thereby preventing chain death by ensuring module-to-module activation. The AHP in neurons of the follower module must overcome both the intrinsic positive imbalance (excitatory > inhibitory) and the positive imbalance projected from the prior module. This requires a longer time in order to achieve higher values of adaptation and slow inhibitory mechanisms. The prolonged activity in module $n+1$ now propagates to module $n+2$ that is exposed to the positive imbalance for a longer time and therefore shows a further augmenting of activity duration.

Activity breadth increased monotonically across the module chain. Parameter exploration shows how broadening depends on excitatory/inhibitory balance (figure 3).

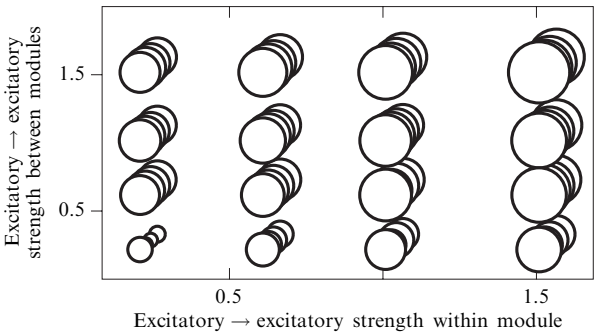

Figure 3. Duration of activity (circle size) in module 10 as a function of excitatory → excitatory strength within module (x-axis), excitatory → excitatory strength between modules (y-axis), and excitatory → inhibitory strength between modules (z-axis—diagonal up and to the right).

Increasing excitation within a module (x-axis) produces increased duration of activity in the final module as this parameter tended to increase the within-module activity duration which then produced further breadth increases along the chain as described below. Increasing excitation from one module to the next (y-axis) also increased broadening owing to the increased ability of a prior module to sustain activity in the follower module. By contrast, excitatory – inhibitory cell projections across modules had relatively little effect except at lowest excitatory – excitatory strengths (lower left corner) where increase in this parameter reduced broadening. Similarly, inhibitory – inhibitory projections (present only within-module) and inhibitory to excitatory projections did not substantially affect broadening (not shown).

Analysis of speed of activity propagation showed that increased speed correlated with increased broadening (figure 4). This is an unusual finding for wave propagation—in many preparations, speed varies inversely with change in the intrinsic time constant of the medium so that signal broadening is accompanied by slowed propagation. In the present case, the increased propagation speed is primarily due to the increased rapidity of response of a follower module seen with increased inter-module excitatory – excitatory projection strength. This inter-module excitatory – excitatory projection strength also correlates with broadening as shown in figure 3. Similarly, intra-module excitatory – excitatory strength could also increase propagation velocity as well as broadening—this parameter led to a more rapid recruitment of excitatory elements within the module which must reach a critical mass before substantial activation will occur in a follower module.

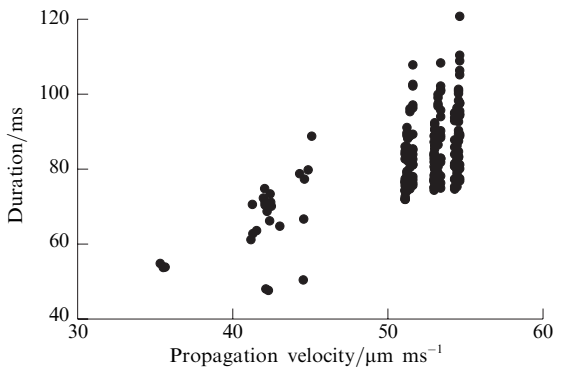

Figure 4. Correlation of duration of activity with propagation velocity.

We looked at multi-electrode recordings from CA1 of hippocampus to determine whether this type of activity broadening was seen in neural tissue. Figure 5 shows activity in 64 electrodes. The third row from the bottom closely follows the pyramidal cell layer with the rightmost electrode near CA3 and the leftmost electrode near subiculum. Activity is initiated with electrode activation in the CA3 stratum radiatum

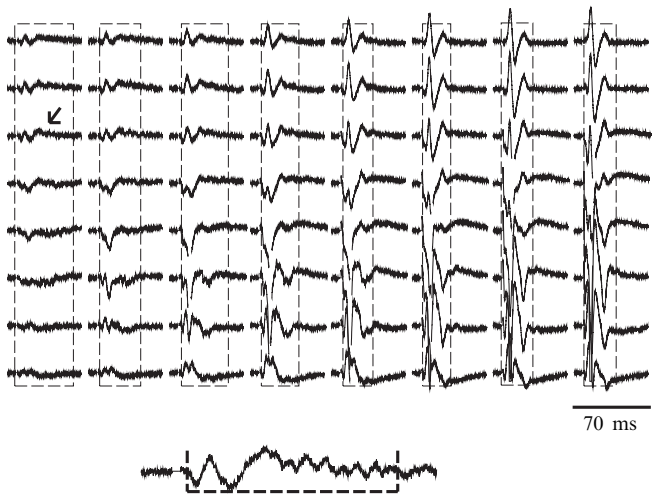

Figure 5. Activity broadens as it travels through disinhibited CA1 slice. Population activity measured at 64 electrodes. Row 3 from bottom follows nearly to pyramidal cell layer. Approximate activity duration is given by the width of each rectangle. Activity is propagating from right to left, from CA3 border to subiculum border. One trace (arrow) is expanded four-fold below. (Stimulation artifact has been removed from all traces.)

and propagates from right to left across the slice. Activation amplitude is reduced substantially across the array from right to left but broadening of activity is also seen. Duration of activity is measured from the first to the last negative-going oscillation in each electrode. The approximate duration of the activity packet in each trace is given by the horizontal length of the dashed rectangle. These rectangles are broader towards the left of the figure, illustrating activity broadening as activity propagates towards subiculum.

In order to estimate duration across a large number of stimulation sweeps, we turned to an automated method to detect initial and final negative-going waves in each trace along the pyramidal cell layer. Out of 400 sweeps, providing $8 \times 400 = 3200$ individual traces, our method was able to interpret 2617 traces. From this we determined an average and standard deviation of onset and offset of activity in each location and compared duration of activity in neighboring locations (figure 6). Duration of activity in the first three locations activated (right side of graph) were not significantly different, averaging 21.7 ms. Activity in the subsequent locations broadened significantly at each

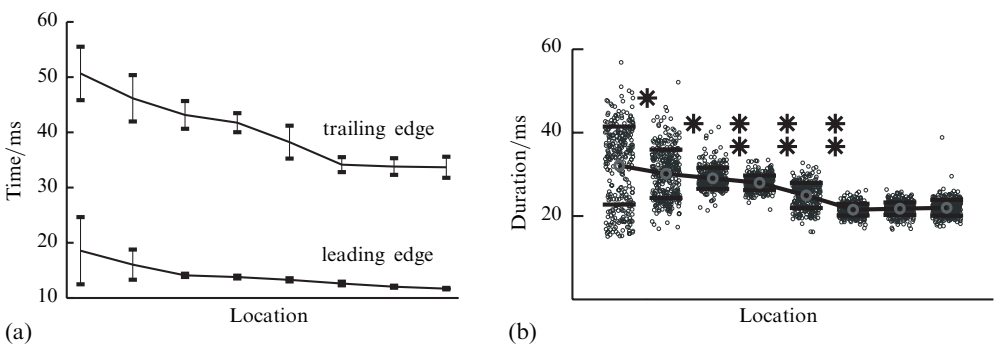

Figure 6. Broadening of activity in CA1 over 400 sweeps. (a) Mean and standard deviation for time of leading edge and trailing edge of activity. (b) Duration of activity. Asterisks show where pairwise Student t-test differences in duration demonstrate $p < 0.01$ (*) and $p < 1 \times 10^{-6}$ (**).

recording point with a gradual increase to a mean duration of 32.1 ms (figure 6b), giving a broadening of approximately 50%.

As activity propagates across the electrode array, the field amplitude is reduced at the same time as it broadens. This is not readily apparent in evaluation of the simulated raster plot (figure 1). Simulated fields from figure 1b are shown in figure 7. It can be seen that there is some slight reduction in amplitude of field associated with broadening across the modules (compare amplitudes at the lower left with those at upper right). Although there are many more spikes in the later locations, they are not as closely synchronized, giving a reduction in population field potential amplitude. Some differences between simulation and slice are apparent. First, the field amplitude for the first location is not particularly high (lower left). Additionally, the amplitude fall off in the simulation is not nearly as great as that in the slice. Our simulated network does not initially synchronize as closely as does the slice.

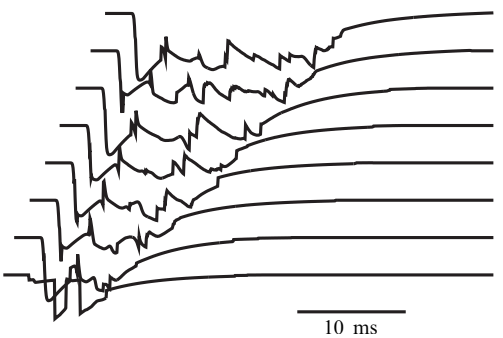

Figure 7. Simulated fields show broadening and reduction in amplitude.

4 Discussion

Whether through synfire chains or rate activation or other mechanism, activity must be transferred without loss from column to column, module to module, area to area. Prior investigators have pointed out the problems of information transfer due to substantial divergence and convergence in cortex and to the presence of other ongoing activity, whether that activity is due to intrinsic noise, to the presence of other information, or to intrinsic dynamics required for homeostatic purposes.

Synfire explosion refers to a spatial spreading of activity broadly in the network, obscuring the desired path of activation. This problem, noted with embedded synfire chains, will tend to obscure information (Mehring et al 2003; Beggs and Plenz 2004). Other groups have identified the type of explosion noted here—temporal rather than spatial—as another problem with synfire chain transmission (Vogels and Abbott 2005; Vogels et al 2005).

The sensorimotor integration required for pre-emptive perception simply adds further length to communication chains and further potential for disruption and confusion. An active perception system requires triggering of mnemonic sketches of motoric associations of an object or scene with subsequent chained activation of other areas based on imagined manipulation (eg the hidden side of the object). If representation broadening (or other signal obscuration) is in fact a constant risk of transmission, then error-correcting mechanisms will need to be utilized at each stage. In the context of an associative memory, such error correction will necessarily involve alteration towards remembered objects or scene (cf the remembered point attractors of a Hopfield network). Here again, the longer one looks, the less one can expect to see.

References

Abeles M, 1991 *Corticonics: Neural Circuits of the Cerebral Cortex* (New York: Cambridge University Press)

Aviel Y, Mehring C, Abeles M, Horn D, 2003 "On embedding synfire chains in a balanced network" *Neural Computation* **15** 1321 – 1340

Beggs J M, Plenz D, 2004 "Neuronal avalanches are diverse and precise activity patterns that are stable for many hours in cortical slice cultures" *Journal of Neuroscience* **24** 5216 – 5229

Carnevale N T, Hines M L, 2006 *The NEURON Book* (Cambridge: Cambridge University Press); also http://www.neuron.yale.edu/neuron/

Gewaltig M O, Diesmann M, Aertsen A, 2001 "Propagation of cortical synfire activity: survival probability in single trials and stability in the mean" *Neural Networks* **14** 657 – 673

Lytton W W, Stewart M, 2005 "A rule-based firing model for neural networks" *International Journal of Bioelectromagnetism* **7** 47 – 50

Lytton W W, Stewart M, 2006 "Rule-based firing for network simulations" *Neurocomputing* **69** 1160 – 1164

Mehring C, Hehl U, Kubo M, Diesmann M, Aertsen A, 2003 "Activity dynamics and propagation of synchronous spiking in locally connected random networks" *Biological Cybernetics* **88** 395 – 408

Vogels T P, Abbott L F, 2005 "Signal propagation and logic gating in networks of integrate-and-fire neurons" *Journal of Neuroscience* **25** 10786 – 10795

Vogels T P, Rajan K, Abbott L F, 2005 "Neural network dynamics" *Annual Review of Neuroscience* **28** 357 – 376

© 2008 a Pion publication

ISSN 0301-0066 (print) ISSN 1468-4233 (electronic)

PERCEPTION
VOLUME 37 2008

www.perceptionweb.com

Conditions of use. This article may be downloaded from the Perception website for personal research by members of subscribing organisations. Authors are entitled to distribute their own article (in printed form or by e-mail) to up to 50 people. This PDF may not be placed on any website (or other online distribution system) without permission of the publisher.